Chapter

Eco-Friendly and Facile Synthesis of Substituted Imidazoles via Nano Zirconia Catalyzed One-Pot Multicomponent Reaction of Isatin Derivatives with Ammonium Acetate and Substituted Aromatic Aldehydes under Solvent Free Conditions

Sundaram Singh and Shivam Bajpai

Abstract

An eco-friendly and highly efficient approach for the synthesis of substituted imidazoles via nano zirconia catalyzed multicomponent reaction of isatin derivatives with ammonium acetate and aromatic aldehydes under solvent-free conditions has been developed. This approach can be mostly applied to medicinal chemistry due of the simple and readily available starting materials, effortless methodology, and biologically active nature of imidazoles. An additional gain of the suggested technique is the reusability of the nano ZrO_2 catalyst.

Keywords: nano ZrO_2 catalyst, multicomponent reaction, imidazole, solvent-free, Isatin

1. Introduction

Imidazole is a "1, 3-diazole" and is classified as an alkaloid. Imidazole (1) refers to the parent compound, whereas imidazoles are a class of heterocycles with similar ring structure, but varying substituents. This ring system is present in important biological building blocks, such as histidine (2), and the related hormone histamine (3). Imidazole can serve as a base and as a weak acid. Many drugs contain an imidazole ring, such as antifungal drugs and Nitroimidazole (4) [1–5].

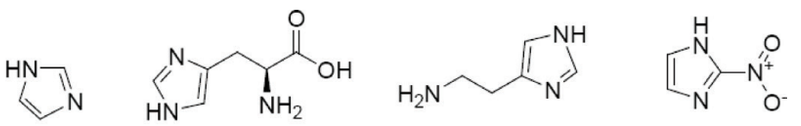

(1) (2) (3) (4)

Imidazole derivatives are mostly used as organic resources [6, 7] and it also plays important roles in various types of biological activities [8, 9]. This multitalented applicability of Imidazole draws attention towards the importance of access to efficient synthetic routes to well-designed and highly substituted imidazole derivatives.

Due to their impressive significance, various synthetic routes have been designed. Substituted imidazoles are generally prepared by microwave irradiated one pot three-component cyclocondensation of a 1, 2-diketone, α-hydroxy ketone or α-ketomonoxime with an aldehyde and ammonium acetate [10–13], ionic liquids [14, 15], refluxing in acetic acid [16], silica sulfuric acid [17, 18], $Yb(OTf)_3$ [19], $Yb(OPf)_3$ [20], iodine [21], $Zr(acac)_4$ [22], $InCl_3{\cdot}3H_2O$ [23], heteropolyacid [24], sodium bisulfate [25], potassium aluminum sulfate (alum) [26], ceric ammonium nitrate (CAN) [27], $(NH_4)_6\,Mo_7O_{24}{\cdot}4H_2O$ [28], zeolite HY/silica gel [29], $ZrCl_4$ [30], polymer-supported $ZnCl_2$ [31] and L-proline [32]. Moreover, they have also been prepared by the addition of substituted amino alcohol to a thioamide and subsequent oxidation with PDC or by the reaction of aryl nitriles and α,α-dilithioarylnitromethanes or by multistep syntheses. *p*-TSA catalyzed synthesis of 2,4,5-trisubstituted imidazoles from 1,2-diketone or α-hydroxyketone, aldehyde and ammonium heptamolybdate tetrahydrate in tetrabutylammonium iodide was given by Khodaei and co-workers [33].

Due to their potential utility, majority of these synthetic routes experience one or more severe disadvantages, such as difficult and intricate work-up and purification, huge amounts of waste materials, strongly acidic conditions, occurrence of side reactions, low yields, high temperature, long reaction time and the use of expensive reagents. Hence, there is a great demand of a highly efficient protocol with mild reaction conditions to synthesize substituted imidazoles.

In recent times, metal nanoparticles are used as heterogeneous catalysts in organic synthesis mainly because they achieve the objectives of green and sustainable chemistry. Recently Scientists have done a lot of work to synthesize precise metal nanoparticles. The new path is the coherent design and synthesis of very active and selective nanocatalysts by controlling the structure and composition of the active nanoparticles among all of them. The easiness of separation, recovery, and reuse of these NPs further enhance their attractiveness as green and sustainable catalysts [3, 34–45].

Recently, nano zirconia (ZrO_2) has attracted considerable attention due to their wide applicability as a heterogeneous catalyst [46–51]. The catalytic activities and selectivities of nano zirconia are highly affected by their crystal phase (monoclinic and tetragonal) [52–54]. ZrO_2 nanoparticle catalyst is a cheap, moisture stable, safe, reusable, and commercially available white powder is of big curiosity to many researchers. It has been revealed from the literature that numerous parallel applications of nano zirconia, as an effective catalyst in green/sustainable synthetic chemistry, have already been reported [55–67].

In view of the above and as a part of our research group to synthesize the biologically active compounds [68–72], it was thought worthwhile to synthesize some novel imidazoles fused with indole nucleus of biocidal interest because the combination of two or more different heterocyclic compounds in a single molecule frequently increases the biocidal profile amazingly. With the aim of getting targeted products, i.e., substituted imidazole a greener "NOSE" (nanoparticles-catalyzed organic synthesis enhancement) approach has been designed under solvent-free conditions.

2. Results and discussion

Imidazole derivatives **4a–s** was synthesized by one pot multicomponent reaction of isatin derivatives **1a–g** with ammonium acetate **2** and substituted benzaldehydes

3a–f in the presence of catalytic amount of ZrO_2 NPs under solvent-free conditions at 110°C, in good to excellent yields (**Scheme 1**).

To optimize the reaction conditions, several parameters were tested. The catalytic efficiency of the ZrO_2 NPs was highly influenced by their amount (mol%). Therefore, a model reaction of isatin with ammonium acetate and benzaldehyde using different amounts of ZrO_2 NPs was carried out (**Table 1**). It has been observed that there is a notable impact of the catalyst on the yield of product and in the absence of catalyst only poor yield was obtained after 120 min (Entry 1, **Table 1**). It was found that product yield is increased with increasing catalyst concentration. Only 5 mol% of catalyst was required to provide 60% yield in 60 min (Entry 2, **Table 1**). The best yield of 88% was obtained with 15 mol% of ZrO_2 NPs (Entry 5, **Table 1**). However, the reaction rate and product yield were not improved by further increase of catalyst concentration (>15 mol%) (Entry 6, **Table 1**).

To optimize the molar proportion of the reactant, the model reaction was carried out using different molar proportions of reactants (**Table 2**). A scrutiny of the table clearly shows that the best result was obtained using isatin, ammonium acetate, benzaldehyde in the molar proportion 1.0:5.0:1.0 at 110°C under solvent free conditions (Entry 5, **Table 2**).

To see the effect of temperature, the model reaction was examined under different temperatures. Obviously, reaction rate and product yield both were increased with enhancing temperature from 50 to 110°C. This study shows that the 110°C was favorable temperature for the multicomponent reaction of isatin with ammonium acetate and benzaldehyde (**Table 3**).

Screening of solvent showed that solvent had a remarkable impact on the yield of product. It was observed that polar solvent provided better yield than nonpolar solvent, but excellent yield was obtained without solvent in smaller time. This may be due to the competitive adsorption of the solvent with the substrate molecule on the catalyst surface; hence reaction under solvent-free conditions gives excellent yield in short reaction time (Entry 5, **Table 4**). Another reason is that the eutectic mixture having uniform distribution of the reactants brings the reacting species in close proximity to react in solvent free condition than in the presence of solvent (Entry 1–4, **Table 4**).

Under the optimized set of reaction conditions, the effect of type of ZrO_2 (nano or bulk) was also examined using model reaction(**Table 5**). This important parameter was studied by using four concentrations 5, 10, 12 and 15 mol% of ZrO_2. These data proved that particle size and surface area would be an important factor for the catalytic efficiency of the ZrO_2 NPs.

The efficiency of the catalytic activity of the ZrO_2 NPs with several other catalysts was compared and is summarized in **Table 6**. The result indicates that ZrO_2 NPs was the best catalyst in terms of mol%, reaction time and percentage yield (**Table 6**).

Under the optimized reaction condition, the scope of this methodology was extended to the reaction of different isatin with a wide range of aromatic aldehydes. The findings reveal that the proposed methodology is equally applicable for the presence of both electron donating as well as electron withdrawing groups at the 5-position of isatin moiety (**Table 7**).

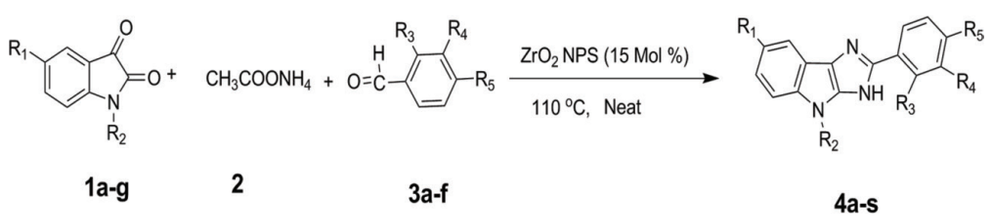

Scheme 1.
Nano ZrO_2 catalyzed synthesis of imidazole derivatives.

Entry	ZrO_2 mol%	Time (min.)	%Yield
1	0	120	23
2	5	60	60
3	10	45	75
4	12	35	82
5	**15**	**30**	**88**
6	20	30	88

Note: Bold values represent optimized reaction condition.

Table 1.
*Effect of catalyst amount (mol%) on yield of the product **4a**.*

Entry	Molar ratio of reactants	%Yield
	Isatin:ammoniumacetate:benzaldehyde	
1	1.0:1.0:1.0	Trace amount
2	1.0:2.0:1.0	35
3	1.0:3.0:1.0	52
4	1.0:4.0:1.0	78
5	**1.0:5.0:1.0**	**88**
6	1.0:6.0:1.0	87
7	1.0:5.0:1.2	87
8	1.2:5.0:1.0	86

Note: Bold values represent optimized reaction condition.

Table 2.
*Effect of molar ratio of substrates on the yield of the product **4a**.*

Entry	Temp. °C	Time	% Yield
1	rt	-	No reaction
2	50	10 h	Trace amount
3	60	6 h	65
4	70	4 h	70
5	80	1.5 h	78
6	90	55 min	84
7	100	45 min	86
8	**110**	**30 min**	**88**
9	120	30 min	88

Note: Bold values represent optimized reaction condition.

Table 3.
*Effect of temperature on the yield of the product **4a**.*

The model reaction was carried out to examine the reusability of the catalyst, After each reaction, catalyst was recovered by filtration, washed, air-dried and reused directly for the next time up to run no. 10.The results showed that there is no obvious loss in product yield in subsequent reuse which proves the reusability and recyclability of ZrO_2 NPs (**Table 8**).

Entry	Solvents	Time	%Yield
1	Ethanol	10 h	68
2	Acetonitrile	10 h	59
3	Xylene	13 h	55
4	Tolune	18 h	52
5	**Solvent free**	**30 min**	**88**

Note: Bold values represent optimized reaction condition.

Table 4.
*Effect of solvents on the yield of the product **4a**.*

Type of ZrO_2	Mol%	% Yield
ZrO_2 (Bulk)	5	42
Surface area: 6.95m^2/g	10	51
Average particle size: 2 μm	12	56
	15	66
ZrO_2 (Nano)	5	59
Surface area: 44.70 m^2/g	10	72
Average particle size: 20 nm	12	84
	15	88

[a]*Reaction condition: Isatin, ammonium acetate & benzaldehyde (1.0, 5.0, 1.0) were stirred at 110°C to produce solid product.*

Table 5.
*Effect of type of ZrO_2 (bulk & nano) on the yield of the product **4a**.*

Type of catalyst	Mol%	Time (min.)	% Yield
Bentonite clay	20	60	55
K-10 clay	20	60	58
PTSA	40	75	45
NH_4Cl	30	75	44
EDTA	40	75	40
Iodine	30	60	53
$Yb(OTf)_3$	25	60	51
TiO_2 (Nano)	20	30	80
ZrO_2 (Nano)	**15**	**30**	**88**

Note: Bold values represent optimized reaction condition.

Table 6.
*Effect of different catalysts on the yield of the product **4a**.*

The following mechanism was proposed for the formation of substituted imidazoles catalyzed by the ZrO_2 NPs is given in **Scheme 2**. The reaction proceeds via the diamine intermediate [X]. Condensation of diamine with isatin derivatives followed by dehydration, and then rearrangement through the imino intermediate [Y] yielded the desired product.

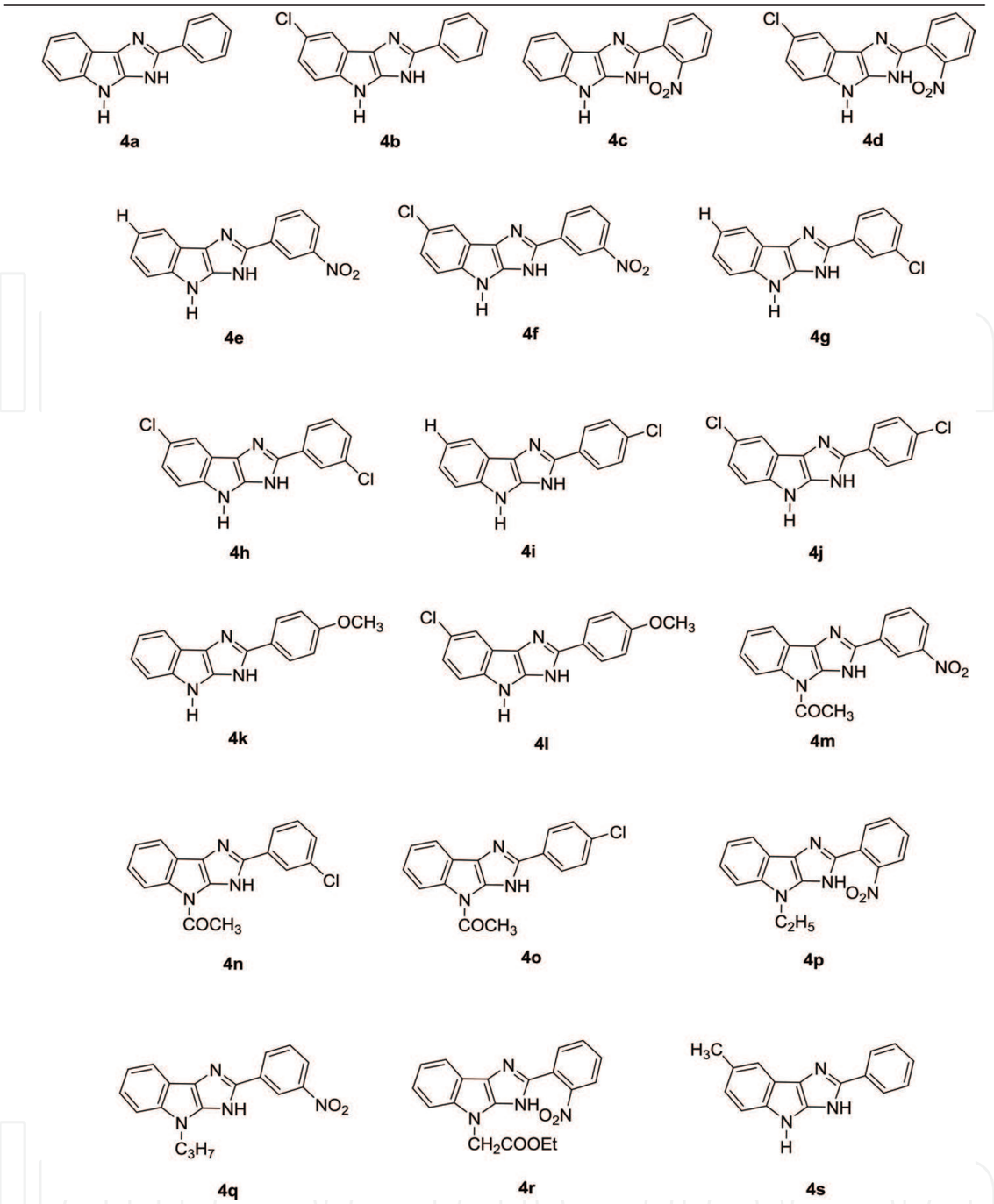

Table 7.
*Synthesis of substituted imidazoles (**4a–s**).*

ZrO_2 NPs were prepared and characterized by FTIR, XRD, SEM and TEM analysis. The BET surface area analyzer was used to calculate the specific surface area of synthesized ZrO_2 NPs.

The molecular nature of the synthesized material was identified by the FT-IR spectrum of the ZrO_2 sample. The FT-IR spectrum of ZrO_2 NPs depends on the nature of the material, preparative procedures used, solid-state structure, and so forth. In FT-IR, a strong absorption peak at about 500 cm^{-1} region is due to the Zr–O vibration, which confirm the formation of ZrO_2 structure while the peak at 751 cm^{-1} is due to stretching vibrations of Zr–O–Zr, prominent peak at 1340 cm^{-1} represents O–H bonding, peak at 1622 cm^{-1} perhaps owing to the adsorbed moisture and peaks at about 2855–2922 cm^{-1} region is due to stretching of O–H groups.

Entry	Number of cycle	%Yield
1	-	88
2	1	88[b]
3	2	87[b]
4	3	86[b]
5	4	83[b]
6	5	80[b]
7	6	80[b, c]
8	7	80[b]
9	8	78[b]
10	9	75[b]
11	10	76[b, c]

[a]*Reaction condition: Isatin, ammonium acetate, benzaldehydes (1.0:5.0:1.0) and ZrO_2 NPs (15 mol%) were stirred at 110°C to produce solid product.*

[b]*The catalyst was washed and dried at 80–90°C for 12 h.*

[c]*ZrO_2 NPs were calcinated at 600°C for 3 h.*

Table 8.
Reusability and recyclability of ZrO_2 NPs catalyst[a].

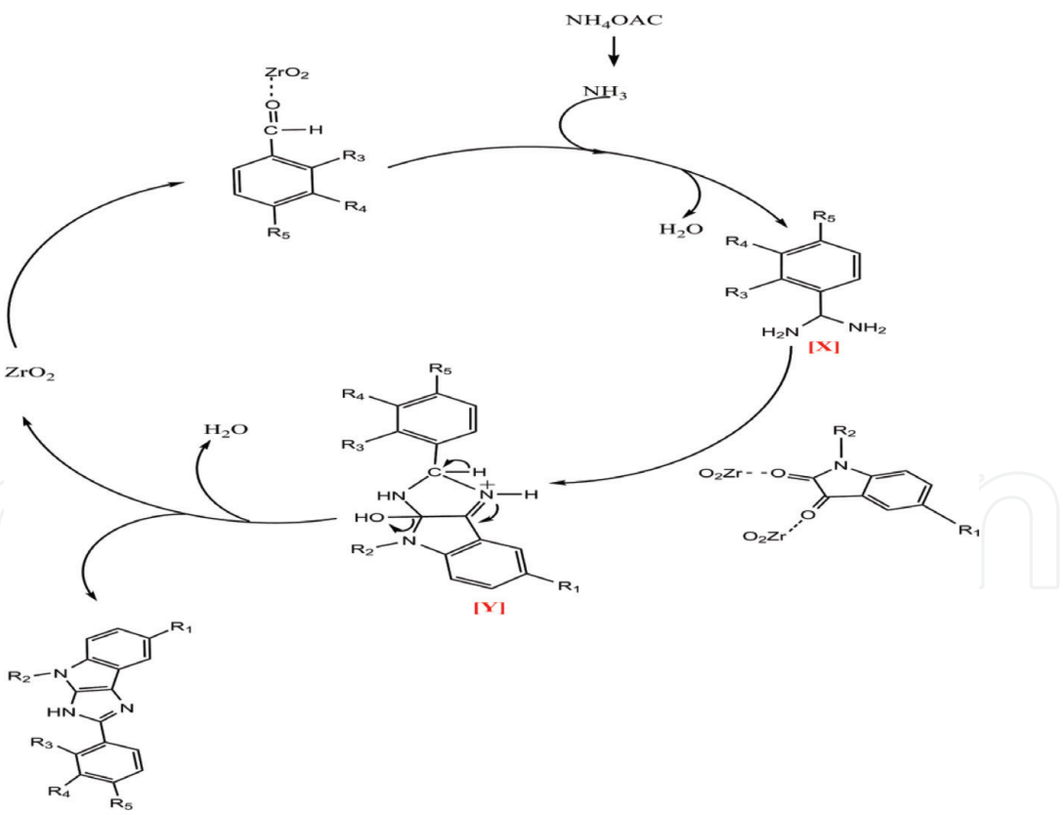

Scheme 2.
*Proposed mechanism for the formation of substituted imidazoles **4a–s**.*

The broad peaks with high intensity in XRD pattern of ZrO_2 NPs indicates that the sample was highly crystalline. The peaks observed at 2θ = 24.2 (011), 28.2 (−111), 31.4 (111), 35.0 (020), 40.5 (−112), 45.0 (211), and 55.4 (−311) are characteristics peaks of monoclinic zirconia (JCPDS card no. 37–1484) while diffraction peak observed at 2θ = 30.3 (101), 50.3 (212) and 60.2 (211) are due to tetragonal

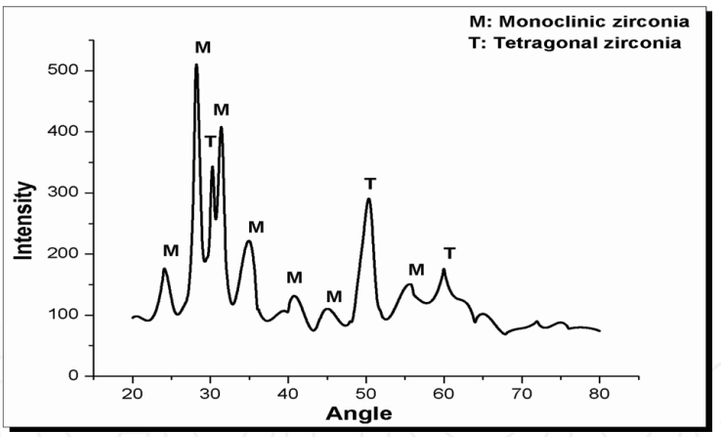

Figure 1.
XRD spectra of ZrO_2 NPs.

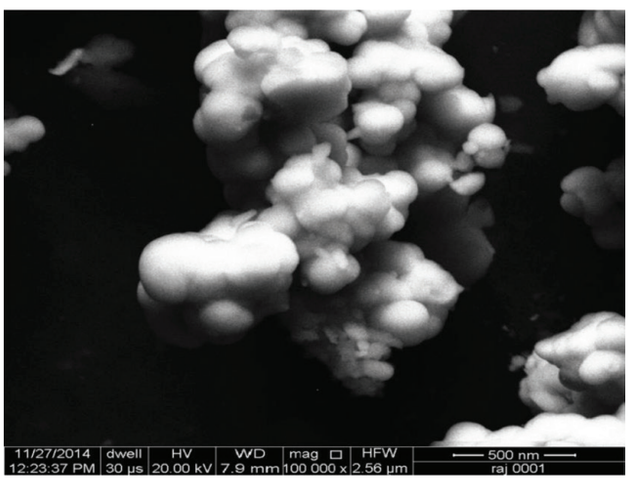

Figure 2.
SEM image of ZrO_2 NPs.

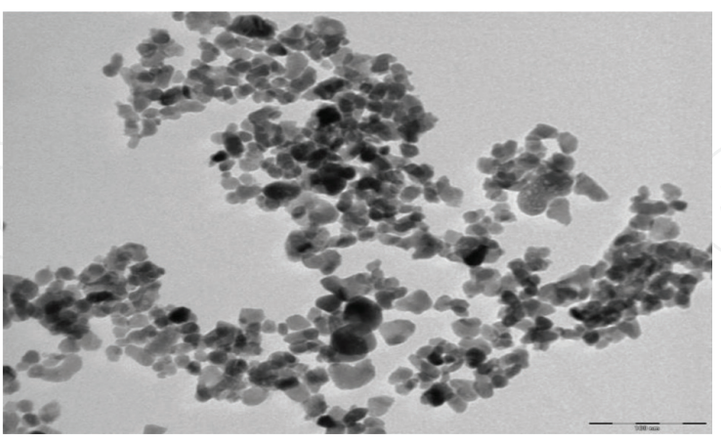

Figure 3.
TEM image of ZrO_2 NPs.

zirconia (JCPDS card no. 79-1769). The broadening of peaks shows the smaller particle size of ZrO_2 NPs **(Figure 1)**.

Morphological studies were done with the help of SEM and TEM analysis of 600°C calcinated ZrO_2 NPs sample that are shown in **Figures 2** and **3**, respectively. SEM analysis shows that NPs are non-homogenous and agglomerated and it also indicates the spherical nature and nano size (nm regime) of the ZrO_2 nanoparticles

but size could be finely decided from TEM. For the purpose, TEM of sample has been shown in **Figure 3**.

As it is clear from TEM micrograph of sample, some agglomeration of the NPs, has been seen due to presence of different m- and t-phases in the sample. It was also observed that the sizes of the particles are of the order 20 nm along with agglomeration.

BET surface area analyzer was used to calculate the surface area of synthesized ZrO_2 NPs by nitrogen absorption which was found to be 44. 70 m^2/g.

3. Experimental

3.1 Typical procedure for the synthesis of ZrO_2 NPs

0.075 M solution of $ZrOCl_2.8H_2O$ was prepared and then precipitated with NH_4OH (25%) with continuous stirring on a magnetic stirrer till the P^H raises in the range of 10–10.5.This resulted in the formation of precipitate of zirconium hydroxide. The precipitate was filtered and washed with double distilled water until traces of chloride ion were completely removed from the filtrate. Complete removal of chloride ion from filtrate was checked by titrating it with $AgNO_3$ solution using potassium chromate as indicator. Now, the precipitate was dried in oven at 80–90°C for 24 h and calcinated at 600°C for 3 h in order to formation of white nano zirconia powder.

3.2 General procedure for the synthesis of substituted imidazoles 4a-s

To a mixture of isatin derivatives **1a–g** (1 mmol), ammonium acetate **2** (5 mmol), substituted aromatic aldehydes **3a–f** (1 mmol), 15 mol% of ZrO_2 NPs was added (**Scheme 1**). The mixture was heated and stirred at 110°C for 30 min. The progress of the reaction was monitored by thin layered chromatography (n-hexane:ethyl acetate, 1:1). After completion, 20 ml acetone was added to the reaction mixture; the catalyst was removed by filtration and washed with xylene and acetone. Then, 50 ml of double distilled water is added to the liquid portion. This resulted in the formation of precipitate of products **4a–s**. The precipitate was filtered, dried and recrystallized with ethanol.

3.2.1 2-Phenyl-3,4-dihydroimidazo[4,5-b]indole (4a)

Brownsolid, **IR (KBr) υ:** 3400, 3209, 3019, 2964, 1660, 1614, 1567, 1484, 1316, 1210, 1171, 1010, 877, 742, 653, 580 cm^{-1}. **1H NMR (300 MHz, DMSO) δ:** 7.80–8.86 (m, 9H, aromatic protons), 9.15 (s, 1H, NH), 9.66 (s, 1H, NH) ppm. **13C NMR (75.45 MHz, DMSO) δ:** 124.0, 126.7, 127.5, 130.2, 130.7, 132.0, 133.7, 135.5, 139.1, 148.2, 160.9 ppm. Anal. Calcd for $C_{15}H_{11}N_3$: C, 77.24; H, 4.74; N, 18.01 Found C, 77.20; H, 4.76; N, 18.03.

3.2.2 7-Chloro-2-phenyl-3,4-dihydroimidazo[4,5-b]indole (4b)

Brownsolid, **IR (KBr) υ:** 3364, 3190, 2981, 2964, 1648, 1609, 1559, 1447, 1311, 1199, 1143, 1019, 872, 744, 651, 566 cm^{-1}. **1H NMR (300 MHz, CDCl3) δ:** 7.51–8.59 (m, 8H, aromatic protons), 9.14 (s, 1H, NH), 9.45 (s, 1H, NH) ppm. **13C NMR (75.45 MHz, CDCl3) δ:** 123.9, 125.7, 128.5, 128.6, 130.3, 130.8, 132.7, 135.0, 137.5, 149.2, 159.4 ppm. Anal. Calcd for $C_{15}H_{10}ClN_3$: C, 67.28; H, 3.78; N, 15.72. Found C, 67.32; H, 3.76; N, 15.70.

3.2.3 2-(2-Nitrophenyl)-3,4-dihydroimidazo[4,5-b]indole (4c)

Brownsolid, **IR (KBr) υ:** 3332, 3201, 2995, 2917, 1658, 1623, 1549, 1485, 1348, 1280, 1176, 1068, 864, 708, 667, 544 cm^{-1}. **1H NMR (300 MHz, DMSO) δ:** 7.61–8.69 (m, 8H, aromatic protons), 9.67 (s, 1H, NH), 9.94 (s, 1H, NH) ppm. **13C NMR (75.45 MHz, DMSO) δ:** 123.8, 126.7, 128.8, 129.8, 130.1, 131.8, 135.4, 135.8, 135.9, 148.3, 160.7 ppm. Anal. Calcd for $C_{15}H_{10}N_4O_2$: C, 64.74; H, 3.62; N, 20.13 Found C, 64.69; H, 3.65; N, 20.14.

3.2.4 7-Chloro-2-(2-nitrophenyl)-3,4-dihydroimidazo[4,5-b]indole (4d)

Brownsolid, **IR (KBr) υ:** 3399, 3229, 2916, 2885, 1645, 1600, 1539, 1457, 1329, 1253, 1162, 1027, 885, 703, 647, 553 cm^{-1}. **1H NMR (300 MHz, CDCl3) δ:** 7.66–8.36 (m, 7H, aromatic protons), 8.96 (s, 1H, NH), 9.50 (s, 1H, NH) ppm. **13C NMR (75.45 MHz, CDCl3) δ:** 123.4, 123.8, 124.8, 127.1, 128.0, 128.6, 129.4, 133.9, 134.1, 134.4, 139.7, 148.7, 150.4, 160.6 ppm. Anal. Calcd for $C_{15}H_9ClN_4O_2$: C, 57.60; H, 2.91; N, 17.91 Found C, 57.51; H, 3.0; N, 17.94.

3.2.5 2-(3-Nitrophenyl)-3,4-dihydroimidazo[4,5-b]indole (4e)

Brownsolid, **IR (KBr) υ:** 3315, 3194, 3066, 2978, 1662, 1623, 1572, 1482, 1353, 1286, 1135, 1025, 832, 797, 661, 542 cm^{-1}. **1H NMR (300 MHz, DMSO) δ:** 7.58–8.55 (m, 8H, aromatic protons), 8.97 (s, 1H, NH), 9.67 (s, 1H, NH) ppm. **13C NMR (75.45 MHz, DMSO) δ:** 122.3, 123.6, 125.2, 127.9, 128.4, 129.7, 130.4, 134.4, 134.5, 135.2, 139.0, 147.6, 161.7 ppm. Anal. Calcd for $C_{15}H_{10}N_4O_2$: C, 64.70; H, 3.63; N, 20.16 Found C, 64.51; H, 3.72; N, 20.23.

3.2.6 7-Chloro-2-(3-nitrophenyl)-3,4-dihydroimidazo[4,5-b]indole (4f)

Brownsolid, **IR (KBr) υ:** 3385, 3211, 3003, 2959, 1646, 1603, 1538, 1458, 1367, 1248, 1122, 1022, 831, 741, 635, 564 cm^{-1}. **1H NMR (300 MHz, DMSO) δ:** 7.77–8.83 (m, 7H, aromatic protons), 9.13 (s, 1H, NH), 9.62 (s, 1H, NH) ppm. **13C NMR (75.45 MHz, DMSO) δ:** 124.0, 126.6, 127.5, 127.6, 130.2, 130.7, 132.0, 133.6, 135.4, 139.1, 148.2, 160.8, 160.9 ppm. Anal. Calcd for $C_{15}H_9ClN_4O_2$: C, 57.61; H, 2.90; N, 17.92 Found C, 57.67; H, 2.90; N, 17.90.

3.2.7 2-(3-Chlorophenyl)-3,4-dihydroimidazo[4,5-b]indole (4g)

Brownsolid, **IR (KBr) υ:** 3405, 3217, 2948, 2909, 1671, 1617, 1568, 1454, 1371, 1283, 1134, 1018, 892, 754, 641, 577 cm^{-1}. **1H NMR (300 MHz, DMSO) δ:** 7.60–8.56 (m, 9H, aromatic protons and 1H, NH), 9.69 (s, 1H, NH) ppm. **13C NMR (75.45 MHz, DMSO) δ:** 123.8, 126.6, 128.8, 128.7, 130.1, 131.0, 131.6, 135.2, 137.0, 148.4, 160.6 ppm. Anal. Calcd for $C_{15}H_{10}ClN_3$: C, 67.30; H, 3.77; N, 15.70 Found C, 67.29; H, 3.75; N, 15.70.

3.2.8 7-Chloro-2-(3-chlorophenyl)-3,4-dihydroimidazo[4,5-b]indole (4h)

Brownsolid, **IR (KBr) υ:** 3398, 3227, 2977, 2893, 1664, 1605, 1551, 1477, 1358, 1242, 1163, 1011, 844, 743, 650, 567 cm^{-1}. **1H NMR (300 MHz, CDCl3) δ:** 7.62–8.31 (m, 7H, aromatic protons), 8.90 (s, 1H, NH), 9.42 (s, 1H, NH) ppm. **13C NMR (75.45 MHz, CDCl3) δ:** 124.1, 125.8, 126.6, 128.6, 129.8, 130.3, 130.7, 133.2, 134.8, 135.2, 139.3, 149.0, 160.5 ppm. Anal. Calcd for $C_{15}H_9C_{l2}N_3$: C, 59.62; H, 3.00; N, 13.91 Found C, 59.52; H, 3.05; N, 13.89.

3.2.9 2-(4-Chlorophenyl)-3,4-dihydroimidazo[4,5-b]indole (4i)

Brownsolid, **IR (KBr) υ:** 3362, 3255, 3015, 2882, 1669, 1620, 1565, 1482, 1375, 1235, 1140, 1026, 890, 777, 663, 526 cm^{-1}. **1H NMR (300 MHz, CDCl3) δ:** 7.48–8.58 (m, 8H, aromatic protons), 9.45 (s, 1H, NH), 10.16 (s, 1H, NH) ppm. **13C NMR (75.45 MHz, CDCl3) δ:** 123.3, 127.8, 127.9, 128.7, 129.7, 134.9, 135.6, 136.2, 149.7, 161.3 ppm. Anal. Calcd for $C_{15}H_{10}ClN_3$: C, 67.30; H, 3.77; N, 15.70 Found C, 67.31; H, 3.75; N, 15.73.

3.2.10 7-Chloro-2-(4-chlorophenyl)-3,4-dihydroimidazo[4,5-b]indole (4j)

Brownsolid, **IR (KBr) υ:** 3386, 3233, 3047, 2960, 1657, 1612, 1558, 1435, 1348, 1282, 1153, 1019, 871, 742, 654, 552 cm^{-1}. **1H NMR (300 MHz, CDCl3) δ:** 7.46–8.54 (m, 7H, aromatic protons), 8.99 (s, 1H, NH), 9.35 (s, 1H, NH) ppm. **13C NMR (75.45 MHz, CDCl3) δ**: 123.9, 125.8, 128.8, 129.8, 130.3, 133.0, 135.2, 136.0, 137.1, 149.1, 159.5 ppm. Anal. Calcd for $C_{15}H_9Cl_2N_3$: C, 59.62; H, 3.00; N, 13.91 Found C, 59.55; H, 3.10; N, 13.90.

3.2.11 2-(4-Methoxyphenyl)-3,4-dihydroimidazo[4,5-b]indole (4k)

Brownsolid, **IR (KBr) υ:** 3351, 3138, 3001, 2944, 2881, 1667, 1619, 1575, 1450, 1371, 1284, 1157, 1021, 863, 743, 654, 534 cm^{-1}. **1H NMR (300 MHz, DMSO) δ:** 4.00 (s, 3H, CH_3), 7.26–8.69 (m, 9H, aromatic protons and 1H, NH), 9.72 (s, 1H, NH) ppm. **13C NMR (75.45 MHz, DMSO) δ:** 56.9, 122.2, 123.2, 125.9, 127.7, 127.4, 127.9, 128.7, 129.0, 129.6, 130.7, 131.2, 131.4, 131.5, 138.5, 139.7, 140.1, 143.9, 145.8, 154.6 ppm. Anal. Calcd for $C_{16}H_{13}N_3O$: C, 72.99; H, 4.98; N, 15.96 Found C, 72.91; H, 5.04; N, 15.95.

3.2.12 7-Chloro-2-(4-methoxyphenyl)-3,4-dihydroimidazo[4,5-b]indole (4l)

Brownsolid, **IR (KBr) υ:** 3370, 3259, 2991, 2911, 1675, 1614, 1558, 1480, 1436 1377, 1291, 1186, 1049, 869, 745, 651, 522 cm^{-1}. **1H NMR (300 MHz, CDCl3) δ:** 3.61 (s, 3H, CH_3), 7.44–8.47 (m, 8H, aromatic protons), 8.58 (s, 1H, NH), 9.36 (s, 1H, NH) ppm. **13C NMR (75.45 MHz, CDCl3) δ:** 61.8, 122.16, 122.29, 124.0, 125.3, 126.6, 130.1, 130.4, 132.3, 133.9, 135.5, 138.5, 148.1, 148.2, 157.8 ppm. Anal. Calcd for $C_{16}H_{12}ClN_3O$: C, 64.54; H, 4.06; N, 14.11 Found C, 64.70; H, 4.00; N, 14.10.

3.2.13 1-(2-(3-Nitrophenyl)imidazo[4,5-b]indol-4(3H)-yl)ethanone (4m)

Brownsolid, **IR (KBr) υ:** 3389, 3266, 2978, 2935, 1694, 1645, 1616, 1571, 1467, 1346, 1224, 1133, 1021, 823, 744, 641, 572 cm^{-1}. **1H NMR (300 MHz, CDCl3) δ:** 1.91 (s, 3H, CH_3), 7.22–8.51 (m, 8H, aromatic protons), 9.40 (s, 1H, NH) ppm. **13C NMR (75.45 MHz, CDCl3) δ:** 23.7, 122.1, 122.4, 123.2, 123.5, 124.8, 127.2, 127.4, 127.6, 128.2, 129.7, 130.1, 130.9, 133.0, 134.1, 134.4, 135.6, 138.0, 141.0, 148.7, 150.4, 160.3, 172.2 ppm. Anal. Calcd for $C_{17}H_{12}N_4O_3$: C, 63.75; H, 3.78; N, 17.49 Found C, 63.68; H, 3.88; N, 17.52.

3.2.14 1-(2-(3-Chlorophenyl)imidazo[4,5-b]indol-4(3H)-yl)ethanone (4n)

Brownsolid, **IR (KBr) υ:** 3367, 3215, 2947, 2923, 1692, 1662 1607, 1580, 1477, 1359, 1272, 1144, 1042, 807, 735, 653, 546 cm^{-1}. **1H NMR (300 MHz, CDCl3) δ:** 1.25 (s, 3H, CH_3), 7.34–8.11 (m, 8H, aromatic protons), 9.36 (s, 1H, NH) ppm. **13C NMR (75.45 MHz, CDCl3) δ:** 23.6, 122.5, 124.1, 125.3, 126.6, 130.1, 130.4, 130.7,

132.3, 133.9, 134.6, 135.5, 138.5, 148.1, 148.2, 157.8, 160.9, 166.2 ppm. Anal. Calcd for $C_{17}H_{12}ClN_3O$: C, 65.92; H, 3.90; N, 13.57 Found C, 66.01; H, 3.95; N, 13.47.

3.2.15 1-(2-(4-Chlorophenyl)imidazo[4,5-b]indol-4(3H)-yl)ethanone (4o)

Brownsolid, **IR (KBr) υ:** 3350, 3285, 3011, 2935, 1685, 1654 1611, 1572, 1485, 1455, 1343, 1284, 1132, 1062, 899, 783, 659, 531 cm^{-1}. **1H NMR (300 MHz, CDCl3) δ:** 1.66 (s, 3H, CH_3), 7.35–8.12 (m, 8H, aromatic protons), 9.37 (s, 1H, NH) ppm. **13C NMR (75.45 MHz, CDCl3) δ:** 23.5, 123.3, 125.6, 127.2, 128.1, 128.4, 128.7, 129.0, 129.2, 129.5, 133.1, 134.3, 134.6, 134.7, 136.4, 137.0, 142.0, 150.5, 160.2, 160.9 ppm. Anal. Calcd for $C_{17}H_{12}ClN_3O$: C, 65.92; H, 3.90; N, 13.57 Found C, 65.99; H, 3.93; N, 13.54.

3.2.16 4-Ethyl-2-(2-nitrophenyl)-3,4-dihydroimidazo[4,5-b]indole (4p)

Brownsolid, **IR (KBr) υ:** 3416, 3199, 3012, 2999, 2942, 2872, 1654, 1607, 1561, 1441, 1453 1351, 1283, 1192, 1021, 861, 741, 657, 526 cm^{-1}. **1H NMR (300 MHz, DMSO) δ:** 1.41–1.45 (t, *J* = 6.6, 3H, CH_3), 4.38–4.45 (q, *J* = 6.9, 2H, CH_2), 7.53–8.63 (m, 8H, aromatic protons), 9.63 (s, 1H, NH) ppm. **13C NMR (75.45 MHz, DMSO) δ:** 12.5, 24.9, 122.1, 122.8, 123.1, 124.6, 127.5, 127.8, 130.2, 130.4, 130.7, 133.5, 134.4, 137.7, 135.4, 136.4, 137.5, 140.7, 148.3, 149.7, 159.9 ppm. Anal. Calcd for $C_{17}H_{14}N_4O_2$: C, 66.66; H, 4.61; N, 18.29 Found C, 66.74; H, 4.65; N, 18.20.

3.2.17 2-(3-Nitrophenyl)-4-propyl-3,4-dihydroimidazo[4,5-b]indole (4q)

Brownsolid, **IR (KBr) υ:** 3400, 3301, 3221, 3135, 3009, 2951, 2912, 2865, 1664, 1616, 1571, 1478, 1422, 1371, 1271, 1181, 1037, 873, 739, 649, 536 cm^{-1}. **1H NMR (300 MHz, CDCl3) δ:** 1.05–1.10 (t, *J* = 6.9, 3H, CH_3), 1.70–1.82 (m, 2H, CH_2), 3.19–3.24 (t, *J* = 6.6, 2H, CH_2), 7.47–8.41 (m, 8H, aromatic protons), 8.94 (s, 1H, NH) ppm. **13C NMR (75.45 MHz, CDCl3) δ:** 10.1, 21.3, 44.0, 121.5, 124.2, 125.2, 125.5, 125.6, 129.3, 136.1, 136.7, 140.5, 150.9, 159.3 ppm. Anal. Calcd for $C_{18}H_{16}N_4O_2$ C, 67.49; H, 5.03; N, 17.49 Found C, 67.44; H, 5.10; N, 17.52.

3.2.18 Ethyl 2-(2-(2-nitrophenyl)imidazo[4,5-b]indol-4(3H)-yl)acetate (4r)

Brownsolid, **IR (KBr) υ:** 3389, 3255, 3129, 3116, 3027, 2969, 2913, 2847, 1735, 1657, 1618, 1569, 1435, 1353, 1264, 1158, 1049, 854, 751, 651, 546 cm^{-1}. **1H NMR (300 MHz, DMSO) δ:** 1.22–1.27 (t, *J* = 7.2, 3H, CH_3), 4.19–4.26 (q, *J* = 6.9, 2H, CH_2), 5.32 (s, 2H, CH_2), 7.37–8.28 (m, 8H, aromatic protons), 9.63 (s, 1H, NH) ppm. **13C NMR (75.45 MHz, DMSO) δ:** 15.0, 52.6, 65.1, 122.3, 123.6, 125.2, 127.9, 128.4, 130.5, 134.0, 135.2, 139.0, 148.3, 149.6, 161.7, 171.0 ppm. Anal. Calcd for $C_{19}H_{16}N_4O_4$: C, 62.63; H, 4.43; N, 15.38 Found C, 62.71; H, 4.51; N, 15.30.

3.2.19 7-Methyl-2-phenyl-3,4-dihydroimidazo[4,5-b]indole (4 s)

Brownish whitesolid, **IR (KBr) υ:** 3398, 3242, 2963, 2931, 1648, 1607, 1559, 1451, 1311, 1232, 1142, 1027, 813, 741, 655, 534 cm^{-1}. **1H NMR (300 MHz, DMSO) δ:** 2.22 (s, 3H, CH_3), 7.55–8.57 (m, 8H, aromatic protons), 9.69 (s, 1H, NH), 10.10 (s, 1H, NH) ppm. **13C NMR (75.45 MHz, DMSO) δ:** 23.9, 122.9, 123.1, 127.7, 128.5, 129.6, 130.2, 130.7, 131.3, 133.3, 136.8, 146.3, 154.1, 161.2 ppm. Anal. Calcd for $C_{16}H_{13}N_3$: C, 77.71; H, 5.30; N, 16.99 Found C, 77.64; H, 5.34; N, 17.02.

4. Conclusion

ZrO_2 nanoparticles have been synthesized and a novel synthetic route has been developed for the multicomponent reaction of isatin derivatives with ammonium acetate and substituted aromatic aldehydes using ZrO_2 nanoparticles under solvent-free conditions. The yields of the products obtained were up to 93% at 110°C. The advantage of the proposed method is its facile reaction conditions; the product can be isolated very easily without the use of column chromatography and the catalyst can be recycled. The simplicity of the presented protocol makes it an interesting alternative to other approaches. The obtained catalyst is expected to contribute to the development of environmentally benign methods and forms a part of nanomaterial chemistry.

A. Appendix

NMR spectra of compound **4a**

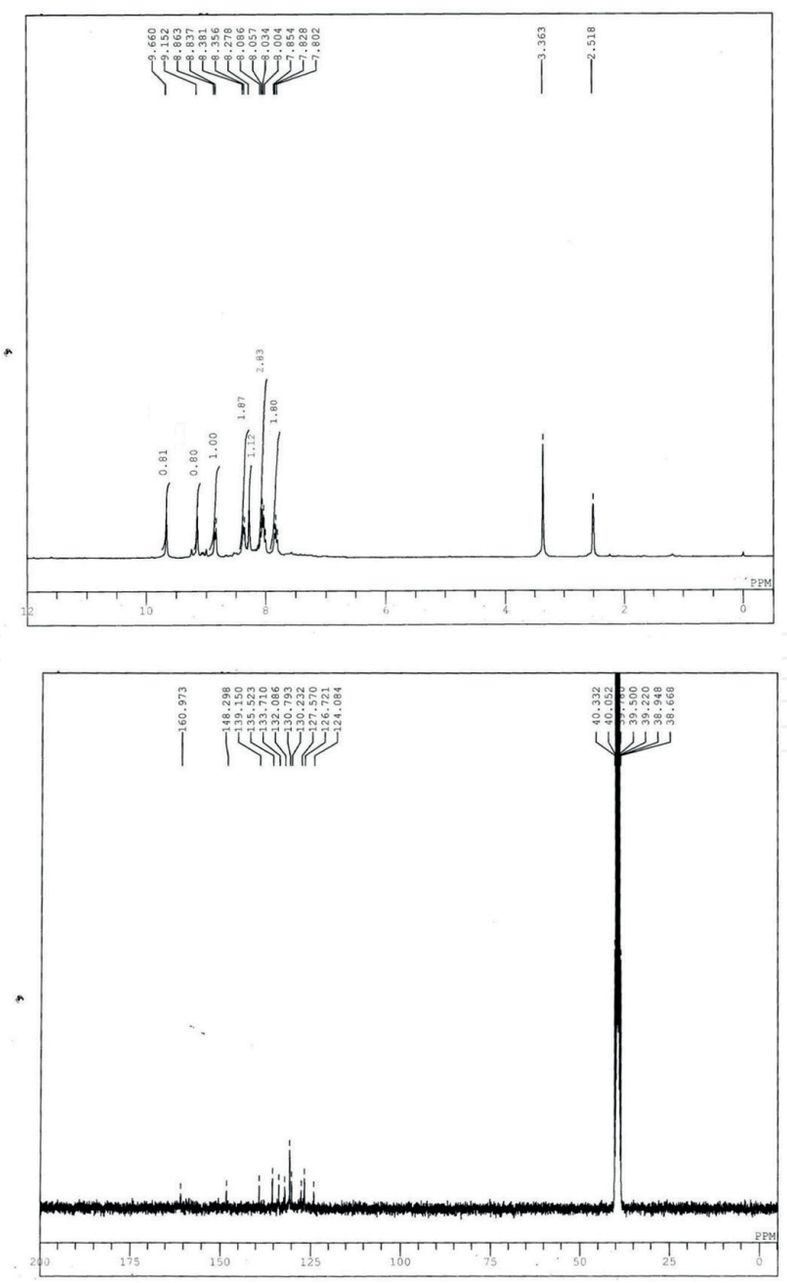

IntechOpen

Author details

Sundaram Singh* and Shivam Bajpai
Indian Institute of Technology (BHU), Varanasi, India

*Address all correspondence to: sundaram.apc@itbhu.ac.in

References

[1] Grimmett M, Katritzky A. In: Rees CW, Katritzky AR, Rees CW, editors. Comprehensive Heterocyclic Chemistry. Vol. 5. New York: Pergamon Press; 1984. pp. 345-456

[2] Grimmett MR. Imidazole and Benzimidazole Synthesis. Cambridge, Massachusetts, USA: Academic Press; 1997

[3] Grunes J, Zhu J, Somorjai GA. Catalysis and nanoscience. Chemical Communications. 2003;**18**:2257-2260

[4] Pozharskii AF, Soldatenkov AT, Katritzky AR. Heterocycles and health. In: Heterocycles in Life and Society: An Introduction to Heterocyclic Chemistry, Biochemistry and Applications. 2nd ed. 1997. pp. 139-183

[5] Brown EG. Ring Nitrogen and Key Biomolecules: The Biochemistry of N-Heterocycles. Berlin, Germany: Springer Science & Business Media; 2012

[6] Gostev F, Kol'tsova L, Petrukhin A, Titov A, Shiyonok A, Zaichenko N. Spectral luminescent properties and dynamics of intramolecular processes in 2,4,5-triarylimidazoles. Journal of Photochemistry and Photobiology, A: Chemistry. 2003;**156**:15-22

[7] Park S, Kwon O-H, Kim S, Park S, Choi M-G, Cha M, et al. Imidazole-based excited-state intramolecular proton-transfer materials: Synthesis and amplified spontaneous emission from a large single crystal. Journal of the American Chemical Society. 2005;**127**:10070-10074

[8] Kruse LI, Ladd DL, Harrsch PB, McCabe FL, Mong SM, Faucette L, et al. Synthesis, tubulin binding, antineoplastic evaluation, and structure-activity relationship of oncodazole analogs. Journal of Medicinal Chemistry. 1989;**32**:409-417

[9] Bunnage ME, Owen DR. TAFIa inhibitors in the treatment of thrombosis. Current Opinion in Drug Discovery & Development. 2008;**11**:480-486

[10] Usyatinsky AY, Khmelnitsky YL. Microwave-assisted synthesis of substituted imidazoles on a solid support under solvent-free conditions. Tetrahedron Letters. 2000;**41**:5031-5034

[11] Sparks RB, Combs AP. Microwave-assisted synthesis of 2,4,5-triaryl-imidazole; a novel thermally induced N-hydroxyimidazole NO bond cleavage. Organic Letters. 2004;**6**:2473-2475

[12] Wolkenberg SE, Wisnoski DD, Leister WH, Wang Y, Zhao Z, Lindsley CW. Efficient synthesis of imidazoles from aldehydes and 1,2-diketones using microwave irradiation. Organic Letters. 2004;**6**:1453-1456

[13] Oskooie HA, Alimohammadi Z, Heravi MM. Microwave-assisted solid-phase synthesis of 2,4,5-triaryl imidazoles in solventless system: An improved protocol. Heteroatom Chemistry. 2006;**17**:699-702

[14] Siddiqui SA, Narkhede UC, Palimkar SS, Daniel T, Lahoti RJ, Srinivasan KV. Room temperature ionic liquid promoted improved and rapid synthesis of 2,4,5-triaryl imidazoles from aryl aldehydes and 1,2-diketones or α-hydroxyketone. Tetrahedron. 2005;**61**:3539-3546

[15] Xia M, Lu Y-d. A novel neutral ionic liquid-catalyzed solvent-free synthesis of 2,4,5-trisubstituted imidazoles under microwave irradiation. Journal of Molecular Catalysis A: Chemical. 2007;**265**:205-208

[16] Chary MV, Keerthysri NC, Vupallapati SV, Lingaiah N, Kantevari S. Tetrabutylammonium

bromide (TBAB) in isopropanol: An efficient, novel, neutral and recyclable catalytic system for the synthesis of 2,4,5-trisubstituted imidazoles. Catalysis Communications. 2008;**9**:2013-2017

[17] Shaabani A, Rahmati A. Silica sulfuric acid as an efficient and recoverable catalyst for the synthesis of trisubstituted imidazoles. Journal of Molecular Catalysis A: Chemical. 2006;**249**:246-248

[18] Shaabani A, Rahmati A, Farhangi E, Badri Z. Silica sulfuric acid promoted the one-pot synthesis of trisubstituted imidazoles under conventional heating conditions or using microwave irradiation. Catalysis Communications. 2007;**8**:1149-1152

[19] Wang L-M, Wang Y-H, Tian H, Yao Y-F, Shao J-H, Liu B. Ytterbium triflate as an efficient catalyst for one-pot synthesis of substituted imidazoles through three-component condensation of benzil, aldehydes and ammonium acetate. Journal of Fluorine Chemistry. 2006;**127**:1570-1573

[20] Shen M-G, Cai C, Yi W-B. Ytterbium perfluorooctanesulfonate as an efficient and recoverable catalyst for the synthesis of trisubstituted imidazoles. Journal of Fluorine Chemistry. 2008;**129**:541-544

[21] Kidwai M, Mothsra P, Bansal V, Somvanshi RK, Ethayathulla AS, Dey S, et al. One-pot synthesis of highly substituted imidazoles using molecular iodine: A versatile catalyst. Journal of Molecular Catalysis A: Chemical. 2007;**265**:177-182

[22] Khosropour AR. Ultrasound-promoted greener synthesis of 2,4,5-trisubstituted imidazoles catalyzed by Zr (acac) 4 under ambient conditions. Ultrasonics Sonochemistry. 2008;**15**:659-664

[23] Sharma SD, Hazarika P, Konwar D. An efficient and one-pot synthesis of 2,4,5-trisubstituted and 1,2,4,5-tetrasubstituted imidazoles catalyzed by $InCl_3 \cdot 3H_2O$. Tetrahedron Letters. 2008;**49**:2216-2220

[24] Heravi MM, Sadjadi S, Oskooie HA, Hekmatshoar R, Bamoharram FF. The one-pot synthesis of 2,4,5-triaryl-imidazoles using heteropolyacids as heterogeneous and recyclable catalysts. Journal of the Chinese Chemical Society. 2008;**55**:1199-1203

[25] Sangshetti JN, Kokare ND, Kotharkar SA, Shinde DB. Sodium bisulfite as an efficient and inexpensive catalyst for the one-pot synthesis of 2,4,5-triaryl-1H-imidazoles from benzil or benzoin and aromatic aldehydes. Monatshefte für Chemie/Chemical Monthly. 2008;**139**:125-127

[26] Mohammadi AA, Mivechi M, Kefayati H. Potassium aluminum sulfate (alum): An efficient catalyst for the one-pot synthesis of trisubstituted imidazoles. Monatshefte für Chemie/ Chemical Monthly. 2008;**139**:935-937

[27] Shaabani A, Maleki A, Behnam M. Tandem oxidation process using ceric ammonium nitrate: Three-component synthesis of trisubstituted imidazoles under aerobic oxidation conditions. Synthetic Communications. 2008;**39**:102-110

[28] Safari J, Khalili SD, Banitaba SH. A novel and an efficient catalyst for one-pot synthesis of 2,4,5-trisubstituted imidazoles by using microwave irradiation under solvent-free conditions. Journal of Chemical Sciences. 2010;**122**:437-441

[29] Balalaie S, Arabanian A, Hashtroudi MS. Zeolite HY and silica gel as new and efficient heterogenous catalysts for the synthesis of triarylimidazoles under microwave irradiation. Monatshefte für Chemie/Chemical Monthly. 2000;**131**:945-948

[30] Sharma G, Jyothi Y, Lakshmi PS. Efficient room-temperature synthesis of tri-and tetrasubstituted imidazoles catalyzed by $ZrCl_4$. Synthetic Communications. 2006;**36**:2991-3000

[31] Wang L, Cai C. Polymer-supported zinc chloride: A highly active and reusable heterogeneous catalyst for one-pot synthesis of 2,4,5-trisubstituted imidazoles. Monatshefte für Chemie/ Chemical Monthly. 2009;**140**:541-546

[32] Samai S, Nandi GC, Singh P, L-Proline SM. An efficient catalyst for the one-pot synthesis of 2,4,5-trisubstituted and 1,2,4,5-tetrasubstituted imidazoles. Tetrahedron. 2009;**65**:10155-10161

[33] Khodaei MM, Bahrami K, Kavianinia I. p-TSA catalyzed synthesis of 2,4,5-triarylimidazoles from ammonium heptamolybdate tetrahydrate in TBAI. Journal of the Chinese Chemical Society. 2007;**54**:829-833

[34] Reetz MT, Westermann E. Phosphane-free palladium-catalyzed coupling reactions: The decisive role of Pd nanoparticles. Angewandte Chemie, International Edition. 2000;**39**:165-168

[35] Ramarao C, Ley SV, Smith SC, Shirley IM, DeAlmeida N. Encapsulation of palladium in polyurea microcapsules. Chemical Communications. 2002:1132-1133

[36] Gladysz JA. Recoverable catalysts. Ultimate goals, criteria of evaluation, and the green chemistry interface. Pure and Applied Chemistry. 2001;**73**:1319-1324

[37] Gladysz JA. Introduction: Recoverable catalysts and reagents perspective and prospective. Chemical Reviews. 2002;**102**:3215-3216

[38] Pacchioni G. Quantum chemistry of oxide surfaces: From CO chemisorption to the identification of the structure and nature of point defects on MgO. Surface Review and Letters. 2000;**7**:277-306

[39] Cox D, Trevor D, Whetten R, Kaldor A. Aluminum clusters: Ionization thresholds and reactivity toward deuterium, water, oxygen, methanol, methane, and carbon monoxide. The Journal of Physical Chemistry. 1988;**92**:421-429

[40] Polshettiwar V, Varma RS. Green chemistry by nano-catalysis. Green Chemistry. 2010;**12**:743-754

[41] Polshettiwar V, Baruwati B, Varma RS. Self-assembly of metal oxides into three-dimensional nanostructures: Synthesis and application in catalysis. ACS Nano. 2009;**3**:28-736

[42] Polshettiwar V, Nadagouda MN, Varma RS. The synthesis and applications of a micro-pine-structured nanocatalyst. Chemical Communications. 2008:6318-6320

[43] Shimizu K, Sato R, Satsuma A. Direct C-C cross-coupling of secondary and primary alcohols catalyzed by a γ-alumina-supported silver subnanocluster. Angewandte Chemie. 2009;**121**:4042-4046

[44] Murugadoss A, Goswami P, Paul A, Chattopadhyay A. 'Green' chitosan bound silver nanoparticles for selective C-C bond formation via in situ iodination of phenols. Journal of Molecular Catalysis A: Chemical. 2009;**304**:153-158

[45] Witham CA, Huang W, Tsung C-K, Kuhn JN, Somorjai GA, Toste FD. Converting homogeneous to heterogeneous in electrophilic catalysis using monodisperse metal nanoparticles. Nature Chemistry. 2010;**2**:36-41

[46] Liu G, Lin Y. Electrochemical sensor for organophosphate

pesticides and nerve agents using zirconia nanoparticles as selective sorbents. Analytical Chemistry. 2005;**77**:5894-5901

[47] Liu S, Han MY. Silica-coated metal nanoparticles. Chemistry - An Asian Journal. 2010;**5**:36-45

[48] Lu J, Zang J, Shan S, Huang H, Wang Y. Synthesis and characterization of core– shell structural MWNT–zirconia nanocomposites. Nano Letters. 2008;**8**:4070-4074

[49] Sholklapper TZ, Radmilovic V, Jacobson CP, Isco SJ, De Jonghe LC. Synthesis and stability of a nanoparticle-infiltrated solid oxide fuel cell electrode. Electrochemical and Solid-State Letters. 2007;**10**:B74-B76

[50] Luo X, Morrin A, Killard AJ, Smyth MR. Application of nanoparticles in electrochemical sensors and biosensors. Electroanalysis. 2006;**18**:319-326

[51] Steiner SA, Baumann TF, Bayer BC, Blume R, Worsley MA, MoberlyChan WJ, et al. Nanoscale zirconia as a nonmetallic catalyst for graphitization of carbon and growth of single-and multiwall carbon nanotubes. Journal of the American Chemical Society. 2009;**131**:12144-12154

[52] Rhodes MD, Bell AT. The effects of zirconia morphology on methanol synthesis from CO and H_2 over Cu/ZrO_2 catalysts: Part I. Steady-state studies. Journal of Catalysis. 2005;**233**:198-209

[53] Stichert W, Schüth F, Kuba S, Knözinger H. Monoclinic and tetragonal high surface area sulfated zirconias in butane isomerization: CO adsorption and catalytic results. Journal of Catalysis. 2001;**198**:277-285

[54] Li W, Yin YQ, Gao RX, Hou RL. Structures and properties of zirconia-supported ruthenium oxide catalysts for the selective oxidation of methanol to methyl formate. Journal of Molecular Catalysis. 1999;**13**:186-192

[55] Yamaguchi T, Tanabe K, Kung YC. Preparation and characterization of ZrO_2 and SO_4^{2-}-promoted ZrO_2. Materials Chemistry and Physics. 1987;**16**:67-77

[56] Yamaguchi T. Application of ZrO_2 as a catalyst and a catalyst support. Catalysis Today. 1994;**20**:199-217

[57] Asakura K, Aoki M, Iwasawa Y. Selective isopentane formation from CH_3OH on a new one-atomic layer ZrO2/ZSM-5 hybrid catalyst. Catalysis Letters. 1988;**1**:395-403

[58] Li W, Liu H, Iglesia E. Structures and properties of zirconia-supported ruthenium oxide catalysts for the selective oxidation of methanol to methyl formate. The Journal of Physical Chemistry B. 2006;**110**:23337-23342

[59] He D, Ding Y, Luo H, Li C. Effects of zirconia phase on the synthesis of higher alcohols over zirconia and modified zirconia. Journal of Molecular Catalysis A: Chemical. 2004;**208**:267-271

[60] Mercera PDL, Ommen VJG, Doesburg EBM, Burggraat AJ, Ross JRH. Zirconia as a support for catalysts: Evolution of the texture and structure on calcination in air. Applied Catalysis. 1990;**57**:127-148

[61] Mercera PDL, Ommen VJG, Doesburg EBM, Burggraat AJ, Ross JRH. Zirconia as a support for catalysts: Influence of additives on the thermal stability of the porous texture of monoclinic zirconia. Applied Catalysis. 1991;**71**:363-391. DOI: 10.1016/0166-9834(91)85092-A

[62] Damyanova S, Grange P, Delmon B. Surface characterization of zirconia coated alumina and silica carriers. Journal of Catalysis. 1997;**168**:421-430

[63] Khodakov A, Olthof B, Bell AT, Iglesia E. Ultrasound-promoted greener synthesis of 2,4,5-trisubstituted imidazoles catalyzed by Zr (acac) 4 under ambient conditions. Journal of Catalysis. 1999;**181**:205-216

[64] Tsipouriari V, Efstathiou A, Zhang Z, Verykios X. Reforming of methane with carbon dioxide to synthesis gas over supported Rh catalysts. Catalysis Today. 1994;**21**:579-587

[65] Maity S, Rana M, Srinivas B, Bej S, Dhar GM, Rao TP. Characterization and evaluation of ZrO_2 supported hydrotreating catalysts. Journal of Molecular Catalysis A: Chemical. 2000;**153**:121-127

[66] Xie S, Iglesia E, Bell AT. Water-assisted tetragonal-to-monoclinic phase transformation of ZrO_2 at low temperatures. Chemistry of Materials. 2000;**12**:2442-2447

[67] Chuah G, Liu S, Jaenicke S, Li J. High surface area zirconia by digestion of zirconium propoxide at different pH. Microporous and Mesoporous Materials. 2000;**39**:381-392

[68] Bajpai S, Singh S, Srivastava V. An easy and efficient protocol for the condensation reaction of isatin and N-substituted isatins with 1,2-diaminobenzene using low cost reusable clay catalyst. Heterocyclic Communications. 2014;**20**:37-39

[69] Bajpai S, Singh S, Srivastava V. Rutile phase nanoTiO2 as an effective heterogeneous catalyst for condensation reaction of isatin derivatives with 1,2-diaminobenzene under solvent free conditions: A greener "NOSE" approach. Arabian Journal of Chemistry. 2014. DOI: 10.1016/j.arabjc.2014.11.037

[70] Bajpai S, Singh S, Srivastava V. Monoclinic zirconia nanoparticle-catalyzed regioselective synthesis of some novel substituted spirooxindoles through one-pot multicomponent reaction in a ball mill: A step toward green and sustainable chemistry. Synthetic Communications. 2017;**47**:1514-1525

[71] Gajaganti S, Bajpai S, Srivastava V, Singh S. An efficient room temperature oxygen radical anion ($O^{2\bullet-}$) mediated one-pot multi-component synthesis of spirooxindoles. Canadian Journal of Chemistry. 2017;**95**:1296-1302

[72] Mishra A, Singh S, Srivastava V. Cerium catalyzed transamidation of secondary amides under ultrasound irradiation: A breakthrough in organic synthesis. Asian Journal of Organic Chemistry. 2018;**7**:1600-1604